

Observation of Novel Instability by using Microwave Imaging Reflectometry in LHD

S. Yamaguchi¹⁾, Y. Nagayama¹⁾, Z.B. Shi²⁾, Y. Kogi³⁾, and A. Mase³⁾

¹⁾National Institute for Fusion Science, Toki 509-5292, Japan

²⁾Graduate University for Advanced Studies, Miura 240-0193, Japan

³⁾Art Science and Technology Center for Cooperative Research, Kyushu Univ., Kasuga 816-8580, Japan

(Received 15 October 2007 / Accepted day 15 October 2007)

A new magnetohydrodynamic (MHD) mode with equally separated higher harmonics has been observed in the Large Helical Device (LHD). The MHD mode appears as the density and magnetic fluctuations in the case of perpendicular ion heating. The poloidal and toroidal mode numbers are $m = 3 / n = 4$ respectively, and the fundamental frequency is 1 ~ 10 kHz, which looks depending on the ion temperature. The density fluctuation is radially localized in the edge region where the rotational transform is nearly $\tau = 4/3$. The feature of the newly observed mode is different from the interchange mode which is frequently observed in LHD.

Keywords: MIR, microwave, imaging, reflectometry, LHD

1. Introduction

The heliontron configuration is one of the promising candidates of the thermonuclear fusion reactor since the plasma is confined in the steady-state without hazardous disruption by using external superconducting coils and a full helical divertor. The Large Helical Device (LHD) is a superconducting heliontron device with the poloidal period number of $L = 2$, the toroidal period number of $M = 10$, the major radius of $R_{ax} = 3.5 \sim 4.1$ m and the averaged minor radius of 0.6 m [1]. The considerable experiment and theoretical efforts have been devoted to the study of instabilities in helical plasmas, however, the present understanding are still not satisfactory.

The recent advance in the microwave technology provides a new generation of the imaging diagnostics in magnetically confined plasma [2-5]. The microwave imaging diagnostics has a potential to obtain 2-D/3-D images of the turbulences and the instabilities with good time and spatial resolutions [6-8]. It brings understanding of the basic physics of the turbulence and the plasma confinement. The microwave imaging reflectometry (MIR) utilizes the radar technique for the measurement of the electron density profiles and its fluctuations by probing the density-dependent cutoff layer in the plasma. The MIR system is under development in the National Institute for Fusion Science, and it can observe the electron density fluctuation with good

sensitivity in LHD [9]. In this paper we will present a newly observed magnetohydrodynamic (MHD) mode, which appears during perpendicular ion heating of neutral beam injection (NBI) or ion cyclotron resonance frequency (ICRF). This mode is accompanied with the equally separated higher harmonics. The experimental setup of the MIR system is described in Section 2, and the newly observed MHD mode is described in Section 3, followed by the conclusion in Section 4.

2. MIR System

Figure 1 shows the schematic view of the MIR system in LHD. The MIR system illuminates the LHD plasma by using the probe wave with frequencies of 53, 66 and 69 GHz in X-mode, and the probe beam is parallel with the diameter of 20 cm. The illumination wave is reflected by the three cutoff layers, which are determined by the local density and the magnetic field. The density fluctuation causes the amplitude modulation and the phase modulation in the reflected beam. The reflected wave is diverged in the case of the density fluctuation with short wavelength. An optical system focuses the reflected wave on the receiver in order to reproduce the microwave image of the fluctuation. The primary imaging mirror with the diameter of 45 cm is installed inside the LHD vacuum vessel. The distance between the mirror and the plasma is about 210 cm. The receiver contains three horn antennas

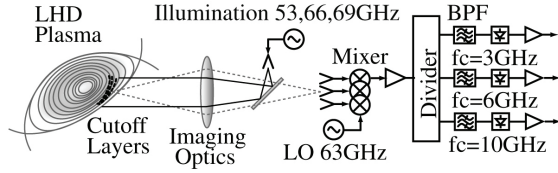


Fig.1 Schematic of the Microwave Imaging Reflectometry (MIR) in LHD.

to detect the microwave image. A pair of receiving antennas is separated by 8.4 cm in the poloidal direction, and another pair by 10.7 cm in the toroidal direction on the cutoff layer. The fluctuation signal is measured by the heterodyne receiver with the sampling time of 1 μ sec. The fluctuation signal of the reflected wave represents the density fluctuation on the cutoff layer in the plasma.

3. Observation

A typical example of this MHD mode is shown in figure 2. The LHD configuration is as follows: $R_{ax} = 3.575$ m, $a = 0.6$ m, $B_t = 2.870$ T, $\gamma = 1.254$ and $B_q = 100\%$. The plasma is basically heated by the co-injected NBI with the power of 8.6 MW and the counter-injected NBI with the power of 3.8 MW. Figure 2 shows time evolutions of the heating power, the beta (β) measured by the diamagnetic diagnostics, the line averaged electron density n_e , the central electron temperature T_e , the central ion temperature T_{i0} and the MIR signal. Figure 2(e) shows the MIR and the magnetic signals showing the mode, which look semi-sinusoidal oscillation.

Figure 3 shows the time evolution of the FFT power spectrum of the MIR signal and the magnetic probe signal. When the plasma is heated by NBI in the co, counter and perpendicular directions, the target mode appears at $t = 1.45$ sec with the sharp spectrum in the FFT power spectrum of the MIR signals. This mode is accompanied with the equally separated several higher harmonics. The same mode appears in the FFT power spectrum of the magnetic fluctuations, however, another mode also appears with the broad spectrum at $t = 1.3$ sec. Right after turning off the perpendicular injected NBI with the power of 3.2 MW at $t = 1.7$ sec, the frequency of the target mode starts dropping, and it looks depending on the ion temperature. Right after turning on the ICRF heating with the power of 1.7 MW, the mode with equally separated several harmonics appears again. So, the perpendicular ion heating looks playing an important role to destabilize this mode. However, the present mode is sometimes observed during only the tangential NBI heating in the case of low density and high temperature plasma.

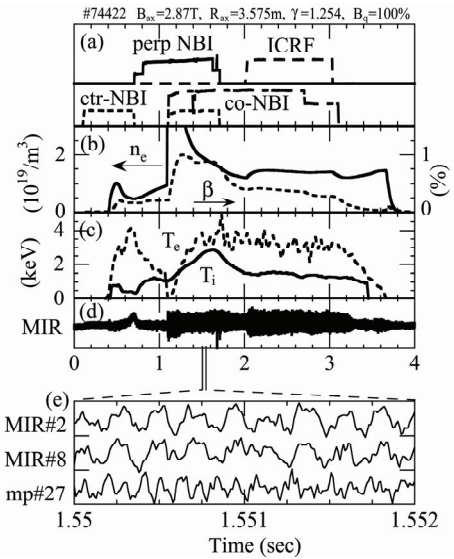


Fig.2 Typical discharge with a newly observed MHD mode. (a) The heating power; (b) the diamagnetic beta (dotted line) and the line averaged electron density (solid line); (c) the central electron temperature (dotted line) and the central ion temperature (solid line); (d) the MIR signal; (e) the MIR signal and the magnetic probe signal in a fast time scale.

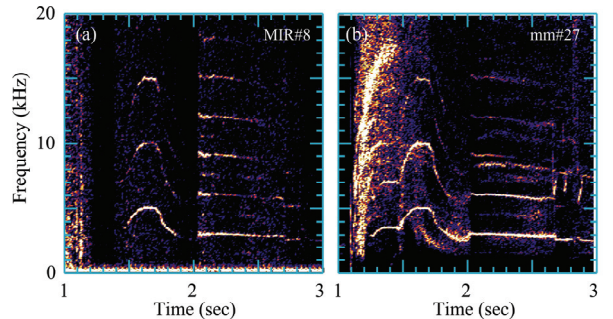


Fig.3 FFT Power spectrum of (a) the MIR and (b) the magnetic probe signal.

The mode numbers is estimated from MIR signals since the magnetic probe signal is not strong enough to identify the mode numbers in the case of low beta. MIR ch.2 and MIR ch.8, which detect the frequency of 63 GHz, are poloidally separated with the distance of about 84 mm at $R = 4.55$ m. It corresponds to the poloidal angle of $\theta = 4.9$ degrees. The phase difference in the fundamental mode can be obtained from the cross power spectrum of these channels. At $t = 1.55$ sec, the phase difference $\delta\theta$ is about 15 degrees. So the poloidal mode number is $m = 3$, and the error is about 1. The mode number of higher

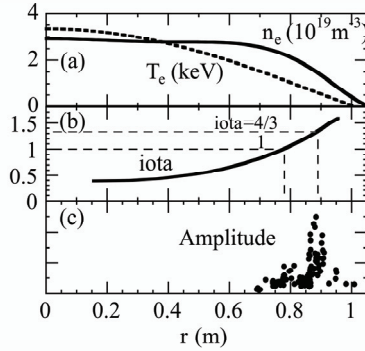


Fig.4 Radial profiles of (a) the electron density (n_e) and temperature (T_e) at $t = 1.6$ sec, (b) the rotational transform, and (c) the amplitude of the fundamental mode of the density fluctuation.

harmonics is proportional to the frequency.

Figure 4(a) shows the radial profile of the electron temperature and the electron density at $t = 1.6$ sec. These are measured with the YAG laser Thomson scattering with 200 spatial channels [10, 11]. By fitting to the 8th order polynomials, smooth T_e and n_e profiles are obtained. The absolute value of the electron density is calibrated by using the 2 mm wave 2-color interferometer [12], of which viewing line has the same configuration of the laser beam of the Thomson scattering in the different port. The radial density profile has the flat top shape and the steep gradient in the peripheral region of the plasma in this case. The cut-off layer for the probe wave in X-mode is obtained from this density profile and the calculated magnetic field in vacuum. Figure 4(b) shows the radial profile of the rotational transform ι . Figure 4(c) shows the amplitude of the fundamental mode between $t = 1.5$ sec and 1.7 sec. These are obtained from 9 discharges of similar operational conditions with slightly different densities. The mode amplitude is localized near $r \sim 0.9$ m where the rotational transform ι is about $4/3$, as shown in Figure 4(c). Here, r is the minor radius in the horizontal port section, defined as $r = R - R_0$ and $R_0 = 3.575$ m in this case. The profile width of the mode amplitude is about 3 cm. At $t = 1.6$ sec the mode amplitude is large on the intermediate cutoff layer of 66 GHz ($r = 0.88$ m). However, it is quite weak on the slightly outer layer of 69 GHz ($r = 0.85$ m) and it disappears on the inner layer of 53 GHz ($r = 0.98$ m). Therefore, the mode is well localized in the radial direction.

The mode presented in this paper is different from known MHD instabilities in LHD. Usual MHD modes observed in LHD are the ideal and the resistive interchange modes [13, 14]. The edge region of LHD plasma is

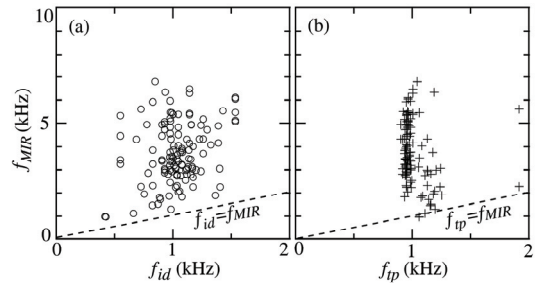


Fig.5 (a) Comparison of the fundamental frequency f_{MIR} vs. the ion diamagnetic frequency f_{id} ; (b) f_{MIR} vs. the toroidal precession frequency f_{pr} in tokamak.

theoretically stable for the ideal interchange mode due to the high shear [15]. As shown in Figure 3, the resistive interchange mode appears in the magnetic fluctuations after the pellet injection at $t = 1.06$ sec. The frequency of the resistive interchange mode increases from $t = 1.1$ sec and decreases from $t = 1.5$ sec. The frequency range of the resistive interchange mode is similar to the target mode. However, features (spectrum and localization) are different. The present mode has sharp spectrum and is localized in narrow space, while the observed resistive interchange mode has a broader spectrum and is not very localized in the radial direction. Actually it spreads more than 12 cm in the MIR measurement. Usual beam driven MHD instabilities are Alfvén eigen modes, and some of them have been observed in LHD [16]. The frequency of TAE mode is more than 100 kHz, and that of GAE mode is the order of 50 kHz. Those frequencies are much higher than that of the present mode.

The frequency characteristic of the target mode is similar to the fishbone oscillations in tokamaks [17]. In the case of tokamak there are two models for explaining the mechanism of the fishbone mode with high frequency branch and low frequency branch. In the high frequency branch the trapped energetic ion destabilizes the mode with the toroidal precession frequency f_{pr} . In the low frequency branch, the energetic ion destabilizes the mode with frequency close to the thermal ion diamagnetic frequency f_{id} . Those frequencies are calculated using the formula for tokamaks [17], as follows:

$$f_{\text{pr}} = \frac{E}{2\pi MrR\omega_0}, \quad f_{\text{id}} = \frac{\nabla p_i}{2\pi e Br R n}$$

where f_{pr} is the toroidal precession frequency of the resonant trapped fast ions, and f_{id} is the finite diamagnetic frequency evaluated at the safety factor $q = 1$ surface.

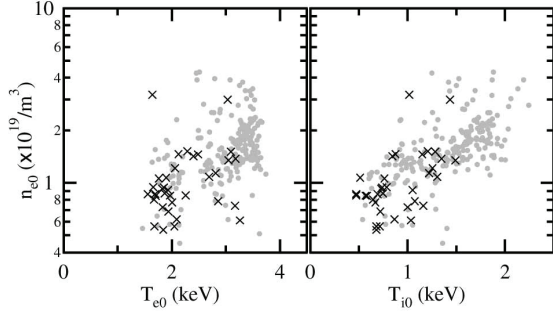


Fig.6 The parameter regions of (a) n_{e0} vs. T_{e0} , (b) n_{e0} vs. T_{i0} , where the mode appears (O) or disappears (X).

Here, E denotes the energy of the ions, $\omega_0 = eB/M$ the gyro frequency and M the mass of the particles, ∇p_i denotes the ion pressure gradient of the plasma bulk and n the plasma density.

In Figure 6, these frequencies are compared with the fundamental frequency of the mode. Here, the f_{id} is calculated by using the density profile and the ion temperature profile, which is measured by the charge exchange spectroscopy. The fundamental frequency is about $f_{MIR} = 1 \sim 7$ kHz, which is several times higher than the ion diamagnetic frequency of $f_{id} = 0.5 \sim 1.6$ kHz. The perpendicular NBI injects the beams with energy of 40 keV, therefore, the toroidal precession frequency around the $\tau = 1$ surface is about $f_{pr} = 1$ kHz. The toroidal precession frequency does not depend on the bulk ion temperature, while the mode frequency increases as T_{i0} increases in the experiment. The fundamental frequency is slightly higher than f_{id} and f_{pr} , however, the clear correlation between the target mode and the low frequency branch of the fishbone mode has not been found yet.

Figure 6 shows the parameter regions of n_{e0} vs. T_{e0} and n_{e0} vs. T_{ei} , where the target mode appears in LHD. In tokamaks, the plasma parameter of the fishbone activity is in the region of high n_e and high T_e [17]. The target mode appears in the cases of high temperature or low density, and is also different from fishbone instability in tokamak. The mode sometimes appears or not with similar plasma parameters. The neutral particle analyzer (NPA) [18, 19] and other diagnostics of LHD suggest that the appearance of the target mode might depend on both the vertical components of the fast ion and the pressure gradient at the resonance surface. The details will be presented soon.

4. Summary

In conclusion, we have observed the new MHD mode with the sharp spectrum and the equally separated higher harmonics by using the MIR in LHD. This is the $m = 3 /$

$n = 4$ mode that is localized in the narrow layer with the width of 3 cm near the $\tau = 4/3$ surface in the edge region. The mode frequency is much less than that of known Alfvén eigen modes, and is similar to the ion diamagnetic frequency. However, we have not obtained a clear evidence of the fishbone instability yet.

Acknowledgement

Technical assistance from S. Sugito and Y. Ito in Department of Engineering and Technical Services of NIFS is gratefully acknowledged. This work is supported by the budgets of the National Institute for Fusion Science (ULPP525), and by the National Institute of Natural Sciences (KEIN0021).

References

- [1] O. Motojima et al., Nuclear Fusion, **45**, S255 (2005).
- [2] C. Lavoron et al., Plasma Phys. Control. Fusion, **38**, 905 (1996).
- [3] E. Mazzucato, Nuclear Fusion, **41**, 203 (2001).
- [4] E. Mazzucato, Plasma Phys. Control. Fusion, **46**, 1271 (2004)
- [5] T. Munsat et al., Rev. Sci. Instrum. **74**, 1426 (2003).
- [6] H. Park et al., Rev. Sci. Instrum. **74**, 4239 (2003)
- [7] H. Park et al., Phys. Rev. Lett. **96**, 195003 (2006).
- [8] A. Mase et al., Rev. Sci. Instrum. **74**, 1445 (2003).
- [9] S. Yamaguchi et al., Rev. Sci. Instrum. **77**, 10E930 (2006).
- [10] K. Narihara, Rev. Sci. Instrum. **72**, 1122 (2001).
- [11] I. Yamada, et al., Rev. Sci. Instrum. **72**, 1126 (2001).
- [12] K. Kawahata, et al., Rev. Sci. Instrum. **70**, 695 (1999).
- [13] S. Sakakibara, et al., Nuclear Fusion, **41**, 1177 (2001).
- [14] S. Sakakibara et al., Plasma Fusion Res. **1**, 003 (2006).
- [15] M. Wakatani, *Stellarator and Heliotron Devices*, (Oxford University Press, New York, 1998).
- [16] K. Toi, et al., Nucl. Fusion, **44**, 217 (2004).
- [17] T. Kass et al., Nucl. Fusion, **38**, 807 (1998).
- [18] T. Ozaki, et al., Rev. Sci. Instrum. **77**, 10E917 (2006).
- [19] E. A. Veshcheyev, et al., Rev. Sci. Instrum. **77**, 10F116 (2006).